زانکۆی سەلاحەدین – هەولیر

Salahaddin University-Erbil

Black Hole that is Relevant to the General Theory of Relativity

Research project

Submitted to the department of (Physics) in partial fulfillment of the requirements for the degree of BCs in (Physics).

By:

Mohammed Mohammedali Rashid

Supervisor:

Dr. Mohammed Issa

2023-2024 A.D **1445 AH** **2723-2724 K**

Abstract

This study explores the relevance of black holes within the framework of the General Theory of Relativity. It investigates their formation, characteristics, and implications, particularly regarding the curvature of spacetime predicted by this fundamental theory of physics. Utilizing a combination of observational techniques and theoretical models, the research analyzes observational data related to black holes. Techniques such as EHT-Imaging, Snapshot-Ring, DoG-HiT, and THEMIS Models are employed to capture images and interpret magnetospheric dynamics. Theoretical models, including the Magnetically Arrested Disk (MAD) and Standard and Normal Evolution (SANE) models, aid in interpreting observational data and predicting black hole event horizons. Recent findings regarding the polarization of the emission ring around Sgr A* provide insights into the magnetic field geometry near supermassive black holes. The concepts such as Hawking radiation and Hawking temperature are discussed, emphasizing the relevance of gravitational-wave astronomy. In conclusion, the study of black holes offers a significant avenue for testing and refining the General Theory of Relativity, contributing crucial insights into the nature of gravity and the structure of the universe.

Acknowledgments

Firstly, all praise and appreciation to **ALLAH** for assisting me in completing this project. Then I would like to thank my supervisor, Dr. Mohammed I. Hussein, for his assistance and guidance in my studies. I would like to thank my loved ones for their attempts and encouragement to assist me. Also, I send my appreciation to everyone who helped my project thus far. And thanks to the University of Salahaddin-Erbil's College of Science, Physics Department.

Contents

Symbol

NAME	SYMBOL
Mass of the sun	$M_{\odot}$
Luminosity of the sun	$L_{\odot}$
Angular momentum	J
Angular radius of the photon ring on the sky	θ
Distance in megaparsecs	D_{Mpc}
Total intensity of the light	I
Linear polarization along the *x*-axis	Q
Linear polarization along the *y*-axis	U
Circular polarization	V
Image-averaged linear polarization fractions across the images	⟨|m|⟩
Hawking temperature	T
Reduced Planck constant	$\hbar$
Boltzmann constant	k
Gravitational constant	G
Rest mass	M_0
Einstein curvature tensor	Gμν
Stress-energy	Tμν

1. Introduction:

The behavior of celestial bodies within the vast expanse of the universe is a testament to the intricate interplay of fundamental forces and the profound principles of general relativity elucidated by Albert Einstein. Just as life follows a cyclical pattern of birth, growth, and eventual demise, so too do massive entities such as stars undergo a life cycle governed by the relentless pull of gravity. It is within this cosmic drama that the enigmatic phenomenon of black holes emerges as a central player. In the cosmic, creation and destruction, stars, fueled by nuclear fusion, blaze with brilliance before succumbing to the inexorable force of gravity. As massive stars reach the end of their life cycle, they collapse inward under their own weight, giving birth to these gravitational behemoths known as black holes. Thus, the life cycle of stars and the principles of general relativity converge in the cosmic phenomenon of black holes, serving as poignant reminders of the awe-inspiring complexity and beauty of the universe. Through the lens of Einstein's groundbreaking theory, we glimpse the profound interconnectedness of all things and the timeless dance of creation and destruction that shapes the cosmos [1].

1.1 Life Cycle of the Stars

A star is a celestial body that fulfills two basic conditions. Firstly, it is self-bound by gravity, Secondly, a star radiates energy that it produces in its interior. A star must have internal forces that prevent it from collapsing under its own gravity. This self-binding force maintains the star's structure and keeps it in a roughly spherical shape [1].

Deviations from sphericity may occur due to factors like rotation, but overall, the gravitational force is radially symmetric. Stars must have an internal energy source that produces the energy they emit as light. In other words, stars shine because they generate their own energy through nuclear fusion processes in their cores. This energy production not only sustains the star's structure but also provides the luminosity that we observe [2].

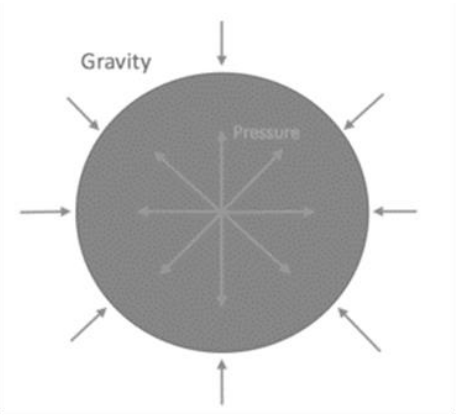

Figure 1 *self-gravity of a star [3].*

This distinguishes stars from planets, which do not have their own internal energy source and merely reflect light from a nearby star, like the Sun. In a stable star, two fundamental forces come into play. Gravity is the force directed inward, trying to compress the star by pulling matter toward its center. In contrast, radiation pressure, generated by nuclear fusion in the star's core, exerts an outward force, preventing gravitational collapse. These forces act in opposing directions, with gravity pulling toward the star's center and radiation pressure pushing away from it, as shown in figure 1 [3].

That makes a star stable is the equilibrium between these forces; neither one is inherently greater than the other in a stable star. This delicate balance allows stars to maintain their shape, size, and overall stability over extended periods. However, as a star progresses through its life cycle, this equilibrium can change. These two conditions distinguish stars from other celestial bodies like planets, comets, and asteroids [4].

In binary system with reliable mass measurements, as figure 2, a strong correlation is observed between the luminosity of main sequence stars and their mass

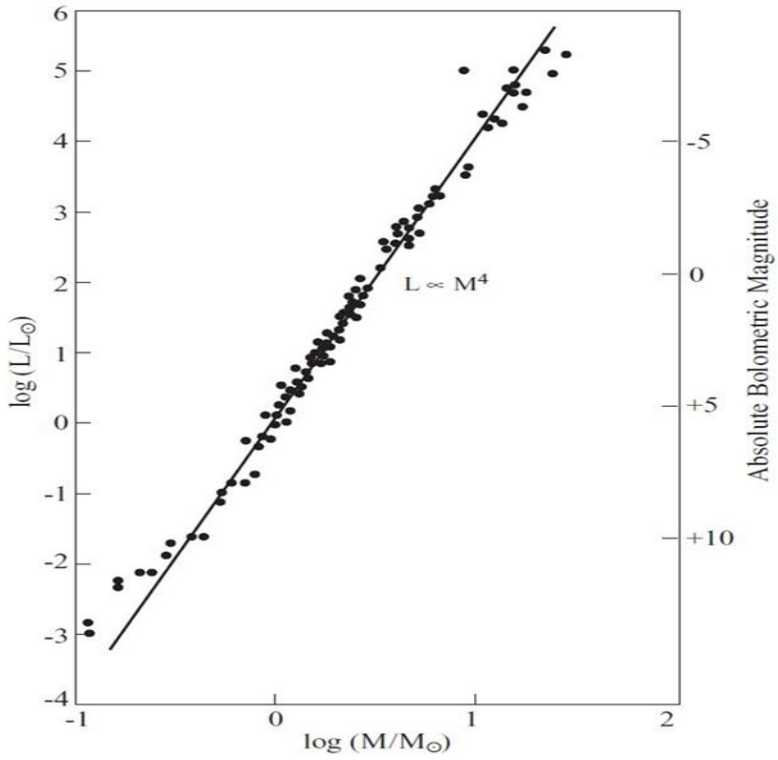

Figure 2 *The empirical mass-luminosity relation for main-sequence stars expresses the absolute luminosity (L) in units of solar luminosity (L_o) as a function of the mass (M) in units of the Sun's mass (M_o). The relation is represented by a straight line, indicating that the luminosity is proportional to the fourth power of the mass [5].*

when plotting luminosity versus mass for the sun (and main sequence star) [5].

The Main Sequence (MS) of stars is a crucial phase in their life cycle, where nuclear fusion processes fully sustain their internal energy needs. This is the stage where stars become optically visible as they contract towards the main sequence,

marking a pivotal moment known as the "stellar birth line" on the HR diagram. The MS is a prominent feature on the Hertzsprung-Russell (HR) diagram, where the majority of stars reside. It is populated by fully mature stars whose energy generation is entirely controlled by nuclear fusion. Stars on the MS exhibit a diverse range of luminosities and colors, with the brightest and bluest stars positioned at the upper left, and the faintest and reddest stars found at the lower right. This region is where solar-type stars spend the majority of their lifetimes, relying on hydrogen fusion as their primary source of energy [2], [5].

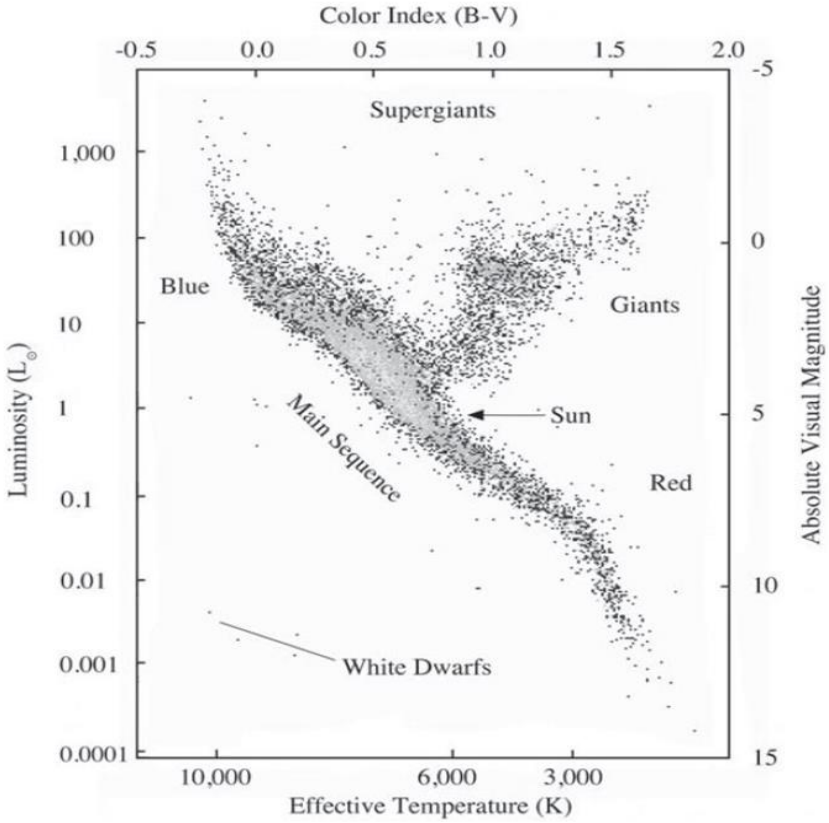

Figure 3 *The Hertzsprung–Russell diagram illustrates the correlation between luminosity and temperature for stars. Main-sequence stars, like our Sun, populate the central band, deriving energy from hydrogen fusion. Evolutionary trajectories are visible, depicting transitions to red giants and eventual white dwarfs. Above the main sequence, rare supergiant and giants are found, while the lower-left corner represents faint white dwarfs. With absolute visual magnitudes and color indices, the diagram provides a comprehensive overview of stellar properties, aiding our understanding of various stages in stellar evolution [1], [5].*

This sequence is characterized by a star's size, temperature, and luminosity. The abundance of elements within a star, such as hydrogen, helium, and heavier elements, is closely linked to its position on the main sequence and, in turn, its atomic number. As a star evolves, its nuclear reactions gradually change the composition of its core, impacting its atomic number and leading to shifts along the main sequence. This dynamic relationship between a star's position on the main sequence and its elemental

abundance is crucial in understanding stellar evolution and the processes that shape the cosmos [5].

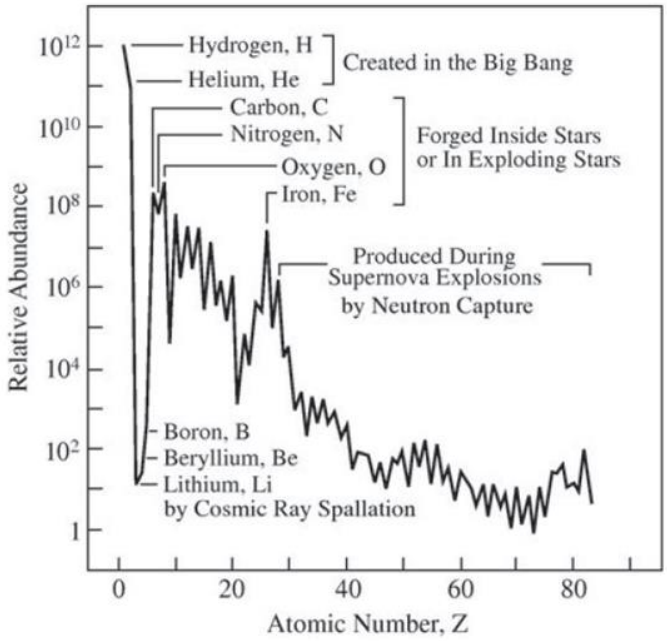

Figure 4 *Abundance and origin of the elements [5].*

As a star ages, it undergoes various stages of evolution. When the majority of hydrogen in its core is processed into helium, the star leaves the main sequence and expands to become a giant, red giant or red supergiant star [1].

A s low to medium-mass stars, when a main sequence star like the Sun exhausts most of its hydrogen fuel in the core, it begins to expand and becomes a giant star. During this phase, the outer layers of the star expand outward, while the core contracts. The increase in the star's size and luminosity is a result of the expansion of the outer layers. This stage is often referred to as a red giant for stars like our Sun. Red giants are cooler than main sequence stars, and their surface temperature decreases as they expand. The outer layers are eventually expelled as a planetary nebula, leaving behind a cooling white dwarf that slowly fades away over billions of years. High-mass stars are on a more cataclysmic trajectory. As the massive star continues to age and consume its nuclear fuel, it undergoes expansion and evolves into a red supergiant. During this phase, the outer layers of the star expand significantly, and the star becomes larger and cooler. Red supergiants are characterized by their large size and reddish appearance [2], [6].

In the core of the red supergiant, nuclear fusion reactions continue, fusing progressively heavier elements. This process can lead to the production of elements up to iron. Iron is unique because it is the element at which nuclear fusion ceases to release energy. Instead, it requires energy input to fuse further. Iron cannot be used as a fuel for nuclear fusion, and as iron accumulates in the core, the star's core becomes unstable. The gravitational pressure becomes overwhelming, causing the core to rapidly collapse [5].

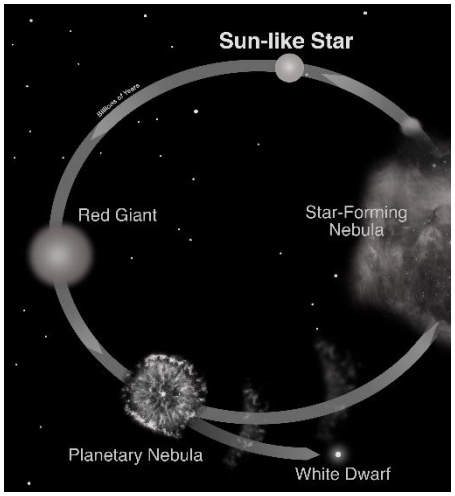

Figure 5 *life cycle of low to medium mass stars [6].*

This stage is known as core collapse. The core collapse happens extremely quickly, in a fraction of a second, and results in a massive release of energy. This sudden

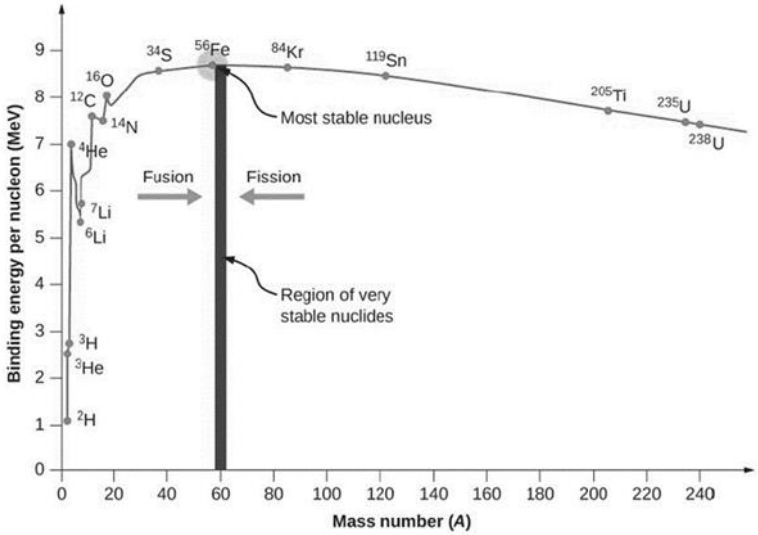

Figure 6 *Binding energy per nucleon versus atomic mass number A [7].*

collapse triggers a powerful supernova explosion. The outer layers of the star are expelled into space at tremendous speeds, while the core itself undergoes further transformation. The core of the massive star can take one of two paths [4].

Firstly, Neutron Star: If the core's mass is below a critical threshold (around 1.4 to 3 times the mass of the Sun), it will form a neutron star. Neutron stars are incredibly dense and composed mainly of neutrons, held together by neutron degeneracy pressure. Secondly, Black Hole: If the core's mass exceeds the neutron star threshold, it will continue collapsing, ultimately forming a black hole. Black holes have intense gravitational fields, and nothing, not even light, can escape their event horizons [5].

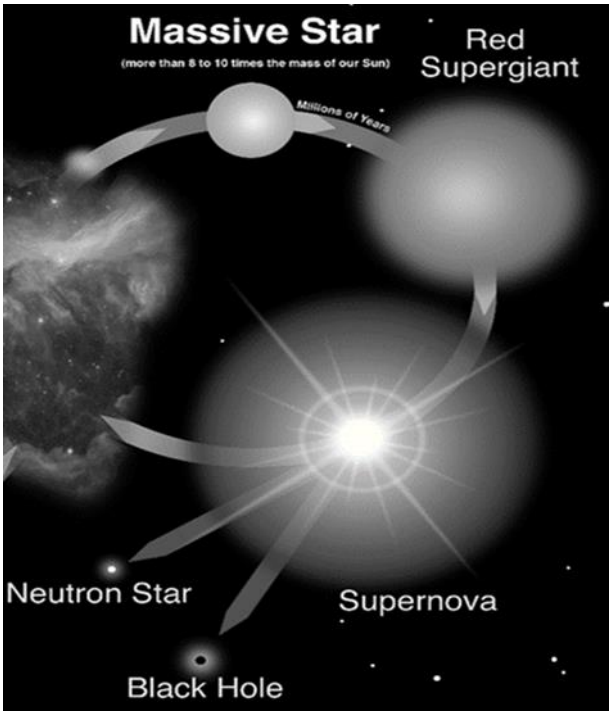

Figure 7 *life cycle of high mass star [6].*

1.2 General relativity

The space-time is a foundational concept that unifies the three spatial dimensions with the temporal dimension, creating a seamless four-dimensional continuum. Within the framework of general relativity, space-time is characterized as a curved manifold influenced by the presence of mass and energy, resulting in curvature. This curvature influences the trajectories of objects and the transmission of light, giving rise to the phenomenon we interpret as gravity [8].

General relativity, formulated by Albert Einstein, revolutionized our understanding of gravity by linking it to the geometry of space-time. In this theory, gravity is not a force but a consequence of the curvature of space-time caused by mass and energy. Objects in this curved space-time follow geodesics, akin to straight lines in curved space. The success of general relativity is evident in its ability to explain diverse phenomena such as gravitational lensing and time dilation in varying

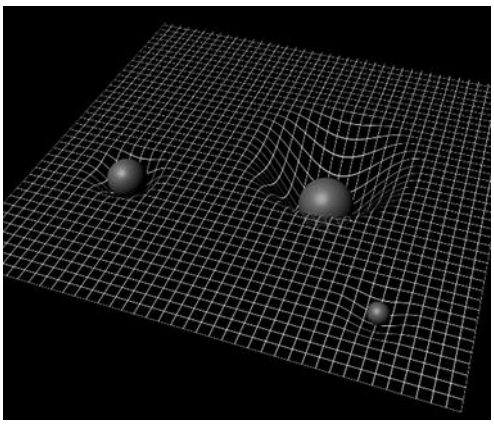

Figure 8 *space-time curvature [10].*

gravitational fields. It has also been crucial in understanding the behavior of astronomical objects such as black holes and the expansion of the universe [8], [9].

General Relativity predicts the existence of the event horizon which is the point of no return beyond which nothing, not even light, can escape the gravitational pull of the black hole which the Event Horizon Telescope (EHT) designed for high-resolution imaging this, and bending of light around the black hole due to its immense gravity, providing a visible ring of light around the black hole's shadow that known as "photo ring" [11], [12].

When thermodynamic principles are applied to black holes within the framework of general relativity, they reveal black holes as thermodynamic systems with properties like entropy and temperature. Additionally, Hawking radiation, predicted by combining quantum mechanics with general relativity near black hole event horizons, demonstrates the intricate interplay between these fundamental theories. Thus, the study of black hole thermodynamics and Hawking radiation enriches our understanding of black hole physics within the context of general relativity, highlighting the deep connections between gravity, thermodynamics, and quantum mechanics[13], [14].

In the context of General Relativity, a singularity refers to a point in spacetime where the curvature becomes infinite. It is a region where the gravitational forces are

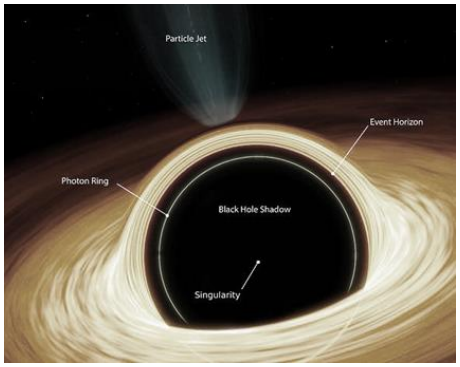

Figure 9 *black hole [16].*

so strong that the laws of physics as we know them break down, and our current understanding of spacetime ceases to be valid [15].

ack hole mergers and gravitational waves have been a significant area of study in astrophysics and gravitational-wave astronomy. Gravitational-wave detectors like LIGO and Virgo have successfully detected mergers of binary black holes by observing the gravitational waves emitted during the coalescence . These detections have confirmed the existence of binary black hole systems and provided crucial data on their masses, spins, and merger rates. Gravitational waves are ripples in spacetime that propagate outward from accelerating masses. These waves are a prediction of general relativity and are generated by violent events in the Universe, such as the merger of black holes or neutron stars. Gravitational waves carry information about the motion of massive objects and the nature of spacetime itself [17].

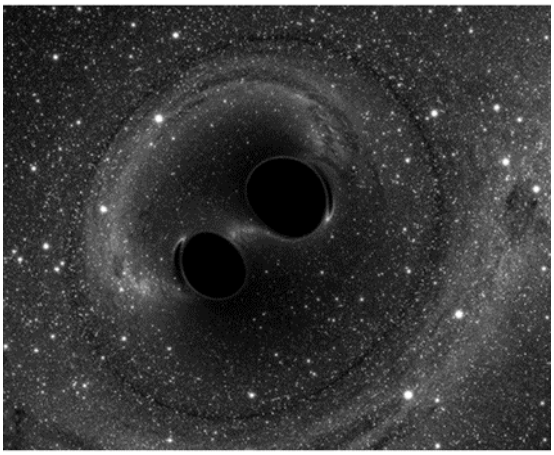

Figure 10 *The black hole binary that produced LIGO's first gravitational-wave signal [15].*

2. Theoretical and Experimental Result

2.1 Event Horizon and Event Horizon Telescope to Photo Ring

The event horizon is a fundamental concept in black hole physics. It is the boundary surrounding a black hole. The Event Horizon Telescope (EHT) aims to capture images of the event horizon of black holes, providing valuable insights into their properties and testing theories of gravity, such as General Relativity . The EHT is a global array of radio telescopes designed to achieve horizon-scale resolution, allowing for the observation of horizon-scale structures around black holes. By studying the shadows cast by black holes on surrounding emission, polarimetric maps, and time-variability, the EHT opens up new avenues for observing and understanding astrophysical black holes. The EHT has demonstrated the feasibility of its project by

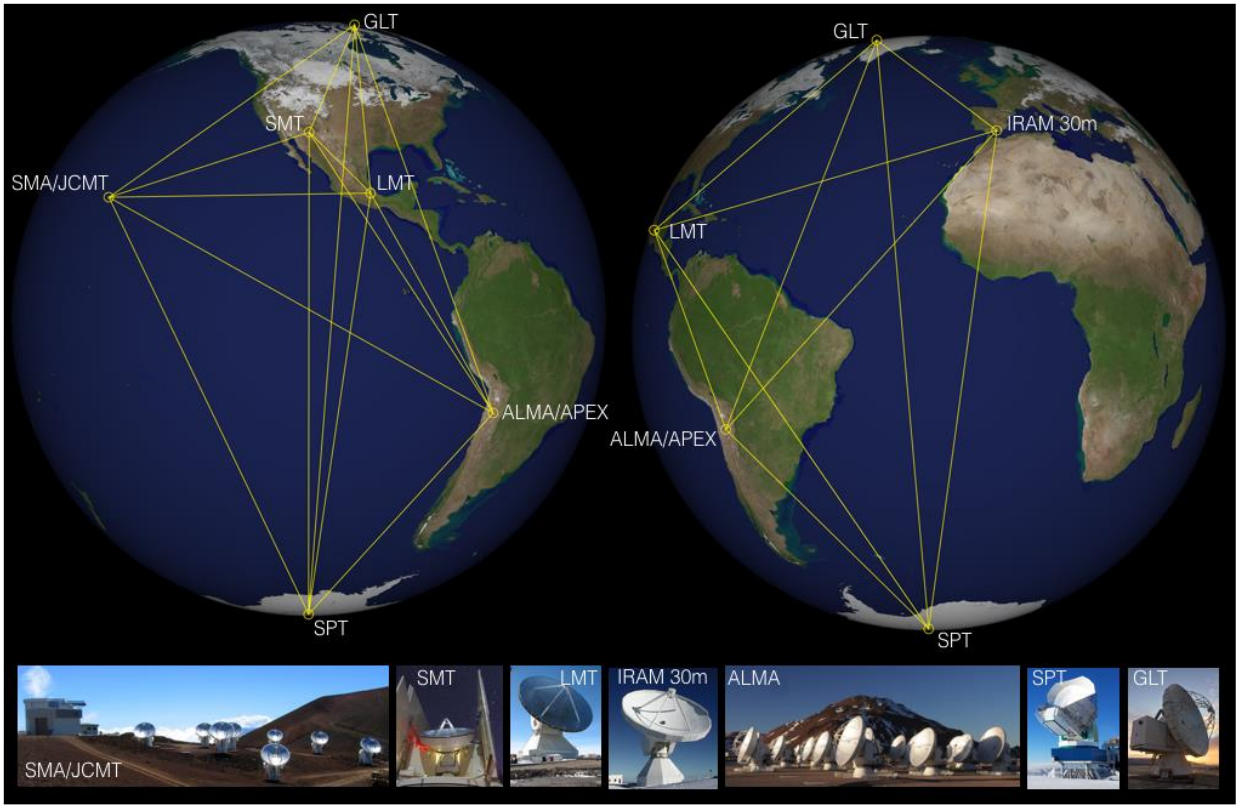

Figure 11: *telescopes around the world that comprise the Event Horizon Telescope [11].*

observing horizon-scale structures at 1.3 mm for the black hole in the center of our Milky Way galaxy, known as Sagittarius A* (Sgr A*), as well as for the black hole in the M87 galaxy. These observations have provided proof of principle for interferometric imaging of horizon-scale structures at millimeter wavelengths, motivating the construction and expansion of the EHT [11].

Surrounding the black hole, the shadow emerges as a distinct dark region amidst the surrounding bright emission, offering astronomers a unique opportunity to study the gravitational effects exerted by the black hole on its immediate vicinity. Observations of the shadow not only provide crucial insights into black hole dynamics but also serve as a testing ground for theories of gravity, including the predictions of

general relativity. In the intricate interplay of light and gravity, the photon ring emerges as a theoretical construct closely tied to the black hole's event horizon. This ring-like structure, formed by photons orbiting the black hole multiple times due to its intense gravitational field, plays a pivotal role in predicting the observable characteristics of black holes. Its dimensions and features are influenced by factors such as the mass and spin of the black hole, as well as the observer's viewing angle, offering the gravitational realm of these enigmatic cosmic entities [11], [12].

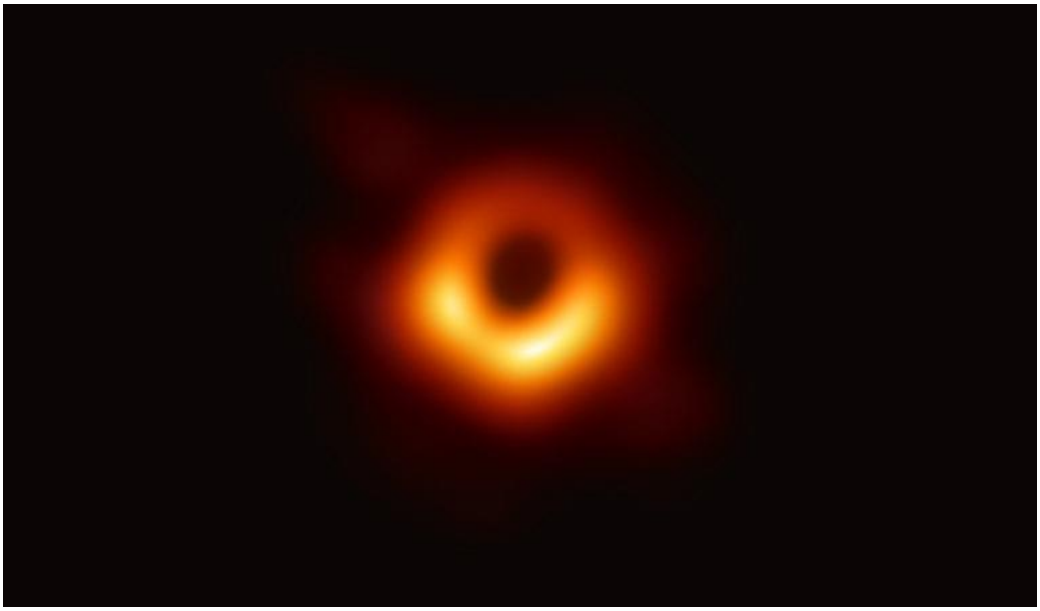

Figure 12 : *supermassive black hole in the center of the galaxy M87 [18].*

2.1.1 Simulation Library

the observations and subsequent image reconstruction were informed by theoretical models based on general relativity, which describes the behavior of spacetime around black holes. These models provided predictions about the appearance of the black hole's event horizon and surrounding emission, guiding the interpretation of the observational data, Magnetically Arrested Disk (MAD) and Standard and Normal Evolution (SANE) models are often employed in theoretical studies of black hole accretion disks to understand the complex interplay between gas dynamics, magnetic fields, and gravitational forces.

Initial data from the Event Horizon Telescope unveils the dynamic shift of the brightest region on the luminous ring encircling the black hole in M87 over time. Scientists conducted a comparison between the actual image, derived from observations conducted in 2017 (positioned at the far right) in figure 13, and simulations representing the appearance of the black hole in earlier years, utilizing preliminary data spanning from 2009 to 2013. These alterations are attributed to the turbulence within the swirling mass of material being drawn into the black hole[19]

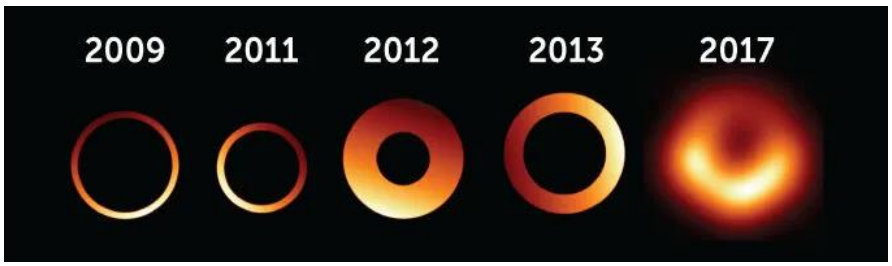

Figure 13 *Initial findings from the Event Horizon Telescope indicate changes in the positioning of the brightest area within the luminous ring surrounding the black hole in M87 over time [19].*

radial coordinate R and the dimensionless spin parameter a* are both essential in describing the spacetime around a rotating black hole, when:

$$R = \sqrt{r^2 + a^2}$$

That (R) is the usual radial coordinate used in spherical coordinates, and (a) is the dimensionless spin parameter of the black hole.

The dimensionless spin parameter a* represents the ratio of the black hole's angular momentum to its mass, and it ranges from 0 for non-rotating black holes to 1 for maximally rotating black holes :

$$a^* = \frac{J}{Mc}$$

Where, (J) is the angular momentum of the black hole, M is its mass, and c is the speed of light. This parameter characterizes how much the black hole is spinning. Inclination i is defined as the angle between the disk angular momentum vector and the line of sight.

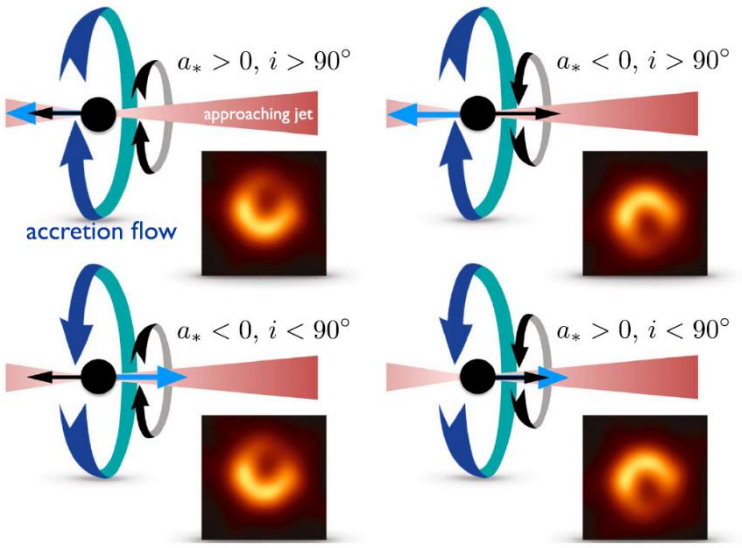

Figure 14 *Illustration of the effect of black hole and disk angular momentum on ring asymmetry [12].*

The equation for the angular radius of the photon ring of a black hole on the sky is a fundamental expression in black hole astrophysics that relates the size of the photon ring to the mass of the black hole and its distance from the observer. This equation is derived from theoretical considerations based on general relativity and the behavior of light in strong gravitational fields near black holes:

$$\theta = \sqrt{27 \frac{GM}{c^2} \frac{D}{D_{Mpc}}}$$

θ *(*ring) is the angular radius of the photon ring on the sky, G is the gravitational constant, M is the mass of the black hole, c is the speed of light, D is the distance to the black hole, D_{Mpc} is the distance in megaparsecs. The data supporting theoretical predictions regarding the photon ring of black holes stem from a blend of observational studies, numerical simulations, and theoretical calculations. Observations, including those from the Event Horizon Telescope (EHT), offer crucial insights into black hole shadows and emissions, enabling comparisons with theoretical models to validate our comprehension of black hole physics The groundbreaking 2019 EHT image of the black hole shadow in M87 provided direct observational confirmation of the photon ring and anticipated shadow features. By aligning observational data with theoretical models based on general relativity and GRMHD simulations, scientists can affirm the harmony between observed black hole properties and predictions from fundamental physics principles. In essence, the data supporting the theoretical framework and equations related to black hole photon rings are derived from a synthesis of observational evidence, numerical simulations, and theoretical analyses. These endeavors collectively aim to elucidate the behavior of light in the extreme gravitational environments surrounding black holes [11],[12].

The decomposition of time-averaged 1.3 mm images into midplane, nearside, and farside components for both MAD and SANE models with $a* = 0.94$ is presented. Each row in the analysis corresponds to a simulation (figure 15) [12]. The decomposition of time-averaged images into midplane, nearside, and farside components in the context of black hole studies is a crucial process that yields valuable insights into accretion flows and emission properties near black holes. These components, each representing distinct regions around the black hole, serve important purposes in understanding the intricate dynamics of material swirling into these cosmic entities. The midplane component, focusing on material along the equatorial plane, provides insights into the structure and behavior of the accretion disk. Similarly, the nearside component, comprising material closer to the observer, offers valuable information about the orientation and geometry of the accretion flow. Meanwhile, the

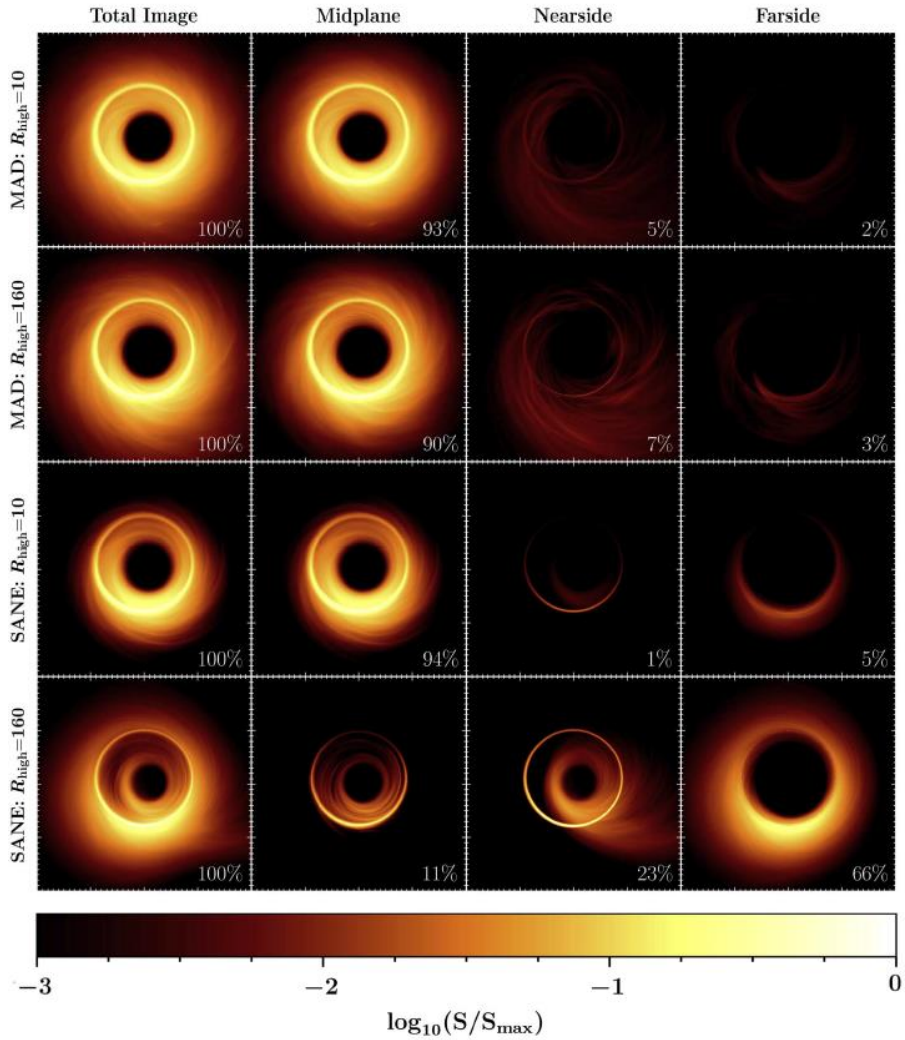

Figure 15 *Decomposition of time-averaged 1.3 mm images, midplane, nearside, and farside components (MAD and SANE models with a* = 0.94) [12].*

farside component, representing material farther from the observer, sheds light on asymmetries and spatial distributions around the black hole [12].

The new findings regarding the polarization of the emission ring around Sgr A* include the first resolved linear and circular polarimetric images of Sgr A*. These findings provide valuable insights into the magnetic field geometry in the vicinity of the supermassive black hole's event horizon [18].

New findings on the polarization of the emission ring around Sgr A* reveal the first resolved linear and circular polarimetric images, offering valuable insights into the magnetic field geometry near the supermassive black hole's event horizon. Linear polarization images display a distinct spiral electric vector polarization angle pattern, with a peak fractional polarization of around 40% in the western part of the emission ring. The models used for linear and circular polarization help to interpret the observed polarimetric features, providing insights into the magnetic field geometry and the physical processes near the supermassive black hole Sgr A* . The image-integrated net linear and circular polarization fractions represent the overall polarization

characteristics of an image, calculated by summing the polarization values of all pixels within the image and normalizing them by the total intensity and measure the image-averaged linear polarization fractions ⟨|m|⟩ across the images :

$$\nu_{net} = \frac{\Sigma_i V_i}{\Sigma_i I_i}$$

$$|m_{net}| = \frac{\sqrt{(\Sigma_i Q_i)^2 + (\Sigma_i U_i)^2}}{\Sigma_i I_i}$$

Stokes parameters **I** (related to the flux density of the light), **Q** and **U** (related to the shape and orientation of the polarization ellipse). Stokes parameter **V** directly relates to the chirality (handedness) of the ellipse representing circular polarization, with the sign of ν determining the direction of rotation of the electric field vector. And Circular polarization images show a modestly polarized dipole structure along the ring, with negative circular polarization in the west and positive polarization in the east. These findings are based on spatially resolved horizon-scale images obtained from Event Horizon Telescope (EHT) observations in April 2017 at 230 GHz. Validation using synthetic data sets ensures the accuracy and reliability of the analysis methods. The equation used to quantify the linear polarization is given by:

$$\langle \vec{P}.\overrightarrow{P_0} \rangle = \frac{Re\,[\langle P\ P_0^* \rangle]}{\sqrt{\langle P\ P^* \rangle}\sqrt{\langle P_0 P_0^* \rangle}}$$

The equation used to quantify the circular polarization is given by:

$$\langle V\ .\ V_0 \rangle = \frac{\langle \nu\ \nu_0 \rangle}{\sqrt{\langle \nu^2 \rangle}\sqrt{\langle \nu_0^2 \rangle}}$$

The related to various models or techniques used in astronomical imaging and data analysis. Here's a brief overview of each:

Ground Truth Average: A baseline used for comparison in analyzing astronomical data.

EHT-Imaging: Techniques for capturing and processing images near black holes using the Event Horizon Telescope.

Snapshot-Ring: Method for studying black hole emission rings by analyzing individual observations.

DoG-HiT: Image processing technique for analyzing features in astronomical data.

THEMIS Models: Computational models used to interpret data from the THEMIS mission, which studies Earth's magnetosphere.

The techniques and models mentioned—EHT-Imaging, Snapshot-Ring, DoG-HiT, and THEMIS Models—contribute to the analysis of observational data related to black holes. By capturing images, analyzing emission rings, enhancing features, and interpreting magnetospheric dynamics, these methods help determine the linear

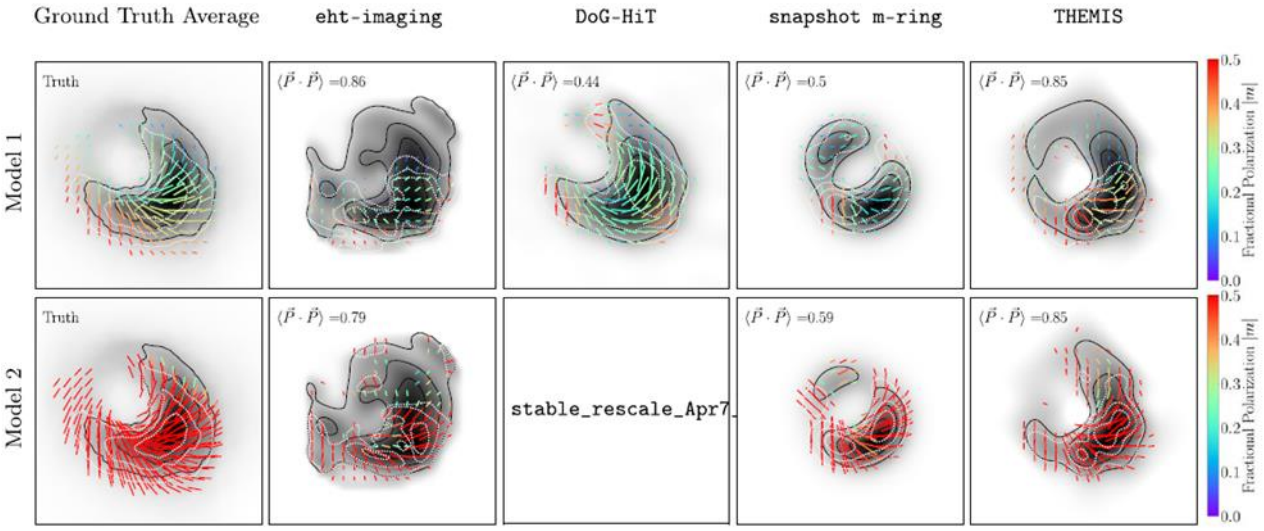

Figure 17 *Linear polarimetric images of synthetic models across all methods [18].*

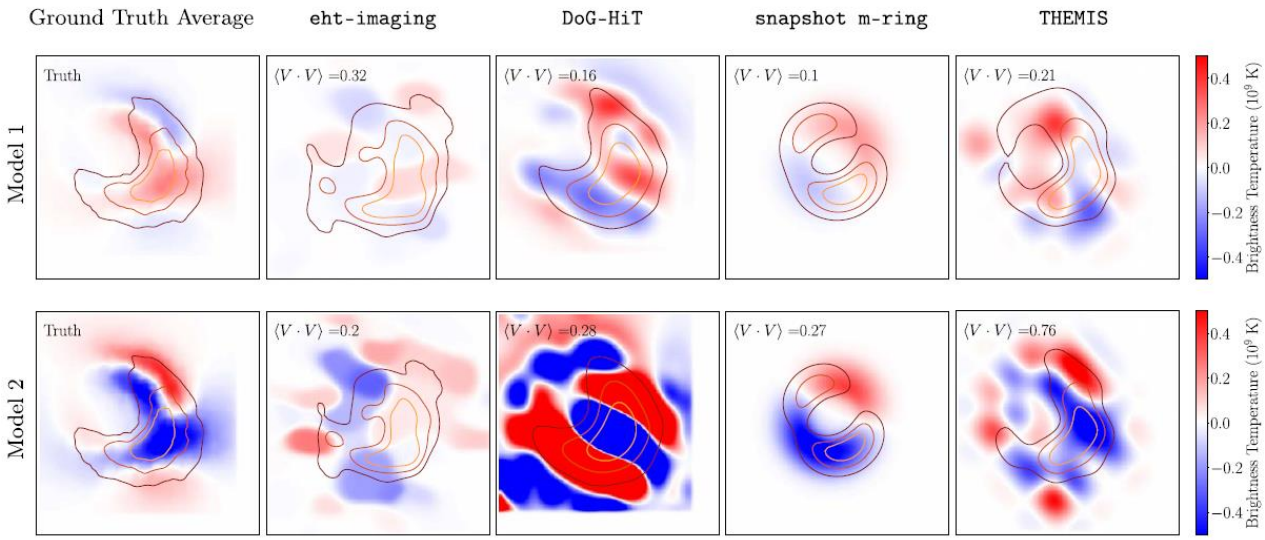

Figure 16 *circular polarimetric images of synthetic models across all methods [18].*

polarization fraction ⟨|m|⟩ across observed regions. Scientists can study both linear and circular polarization fractions across observed regions, facilitating a comprehensive understanding of polarization properties near black holes.

In Figures 16 and 17, the average of the four method images combining bands and days presented. The averaging process is conducted independently for each Stokes intensity distribution. It is observed that the average image is lower than those of individual methods. The selection of this image represents a conservative approach towards depicting the comprehensive linear polarization structure of Sgr A*. Meanwhile,

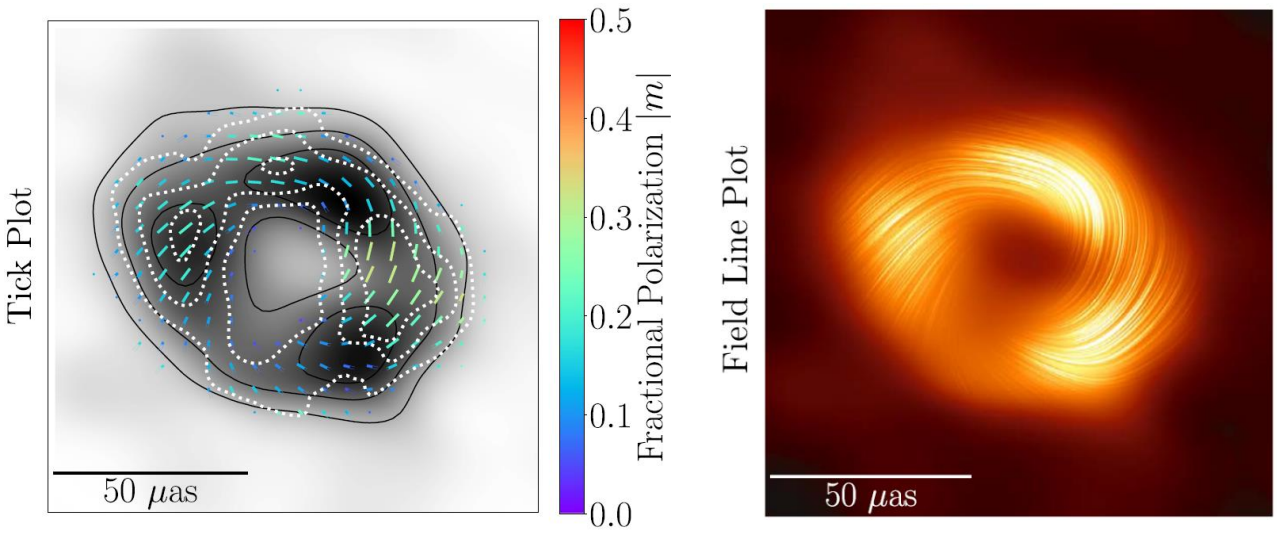

Figure 18 *On the left side, there is a depiction of the linear polarization image of Sagittarius A*. This image represents the average linear polarization structure reconstructed from observations made by the Event Horizon Telescope on April 6 and 7, 2017. On the right side, there is a visualization of polarization "field lines" overlaid on a total intensity image [18].*

individual method images serve the purpose of facilitating quantitative comparisons and theoretical interpretations [18].

2.2 Thermodynamics

according to the concept of Hawking radiation proposed by physicist Stephen Hawking, black holes can emit thermal radiation due to quantum effects near the event horizon. This radiation is associated with a theoretical temperature known as the Hawking temperature [15].

The derivation of the Hawking temperature is based on utilizing the Schwarzschild solution, which characterizes the gravitational field around non-rotating spherical masses like black holes. This solution, stemming from Einstein's equations for vacuum in general relativity, forms the foundational framework for understanding spacetime curvature, that given by:

$$T = \frac{\hbar c^3}{8\pi k G M}$$

Where; T is the Hawking temperature, $\hbar$ is the reduced Planck constant, c is the speed of light in vacuum, k is Boltzmann constant, G is the gravitational constant, and M is the mass of the black hole.

Black holes can spin at velocities ranging from 50% to 99% of the speed of light. Consequently, their mass does not remain constant but varies with velocity, as suggested by Albert Einstein's special theory of relativity:

$$M = \frac{M_0}{\sqrt{1 - v^2/c^2}}$$

M_0 is the rest mass and ν be the spinning velocity of black holes. Since ν/c:

$$\frac{v}{c} < 1 \,,\, \left(\frac{v}{c}\right)^2 << 1 \,,\, \left(\frac{v}{c}\right)^4 <<< 1 \,,\, \left(\frac{v}{c}\right)^6 <<<< 1$$

is clear that the terms of higher power can be neglected and M be:

$$M = M_0 \left[1 + \frac{1}{2}\,(v/c)^2\right]^{-1}$$

$$T = \frac{1}{8\pi M_0} \left[1 - \frac{1}{2}\,(v/c)^2\right]^{1}$$

The relativistic Hawking temperature of black holes is lower than the Hawking temperature of black holes, indicating a decrease in the black hole's temperature as its velocity increases.

To determine the rate at which the temperature of black holes changes relative to velocity, it is differentiated with respect to velocity *v*:

$$\frac{dT}{dv} = \frac{v}{8\pi M_0}$$

$$\left|\frac{dT}{dv}\right| = \frac{v}{8\pi M_0}$$

$$\left|\frac{dT}{dv}\right| \alpha v$$

The equation above illustrates that for highly dense objects such as black holes, the rate of change in temperature with respect to velocity is directly proportional to the spinning velocity of the black hole, whether it is of lower velocity or comparable to the speed of light.

The equation above illustrates that for highly dense objects such as black holes, the rate of change in temperature with respect to velocity is directly proportional to the spinning velocity of the black hole, whether it is of lower velocity or comparable to the speed of light.

Table 1 *The rate of change of temperature of black holes [20].*

S. No	% Spinning velocity of black holes of velocity of light	Spinning velocity of black holes of velocity of light (m/s)	$\left\|\frac{dT}{dv}\right\|$			
			For M = 5M0	For M = 10 M0	For M = 15 M0	For M = 20 M0
1	5%	0.15 × 108	0.60012 × 10−25	0.30006 × 10−25	0.20004 × 10−25	0.15003 × 10−25
2	10%	0.30 × 108	1.20024 × 10−25	0.60012 × 10−25	0.40006 × 10−25	0.30006 × 10−25
3	20%	0.60 × 108	2.40048 × 10−25	1.20024 × 10−25	0.80016 × 10−25	0.60012 × 10−25
4	30%	0.90 × 108	3.60072 × 10−25	1.80036 × 10−25	1.20024 × 10−25	0.90018 × 10−25
5	40%	1.20 × 108	4.80096 × 10−25	2.40048 × 10−25	1.60032 × 10−25	1.20024 × 10−25
6	50%	1.50 × 108	6.00120 × 10−25	3.30006 × 10−25	2.200060 × 10−25	1.50030 × 10−25
7	60%	1.80 × 108	7.20144 × 10−25	3.60072 × 10−25	2.40048 × 10−25	1.80036 × 10−25
8	70%	2.10 × 108	8.40168 × 10−25	4.20084 × 10−25	2.80038 × 10−25	2.10042 × 10−25
9	80%	2.40 × 108	9.60192 × 10−25	4.80096 × 10−25	3.20064 × 10−25	2.40048 × 10−25
10	90%	2.70 × 108	10.80216 × 10−25	5.40108 × 10−25	3.60072 × 10−25	2.70054 × 10−25
11	99%	2.97 × 108	12.00236 × 10−25	6.00120 × 10−25	4.30080 × 10−25	3.00060 × 10−25

Table 2 *The rate of change of temperature of black holes [20].*

S. No	% Spinning velocity of black holes of velocity of light	Spinning velocity of black holes of velocity of light (m/s)	$\left\|\frac{dT}{dv}\right\|$			
			For M = 106M0	For M = 107M0	For M = 108M0	For M = 109M0
1	50%	1.50 × 108	3.000067 × 10−30	3.000067 × 10−31	3.000067 × 10−32	3.000067 × 10−33
2	55%	1.65 × 108	3.300739 × 10−30	3.300739 × 10−31	3.300739 × 10−32	3.300739 × 10−33
3	60%	1.80 × 108	3.600806 × 10−30	3.600806 × 10−31	3.600806 × 10−32	3.600806 × 10−33
4	65%	1.95 × 108	3.900873 × 10−30	3.900873 × 10−31	3.900873 × 10−32	3.900873 × 10−33
5	70%	2.10 × 108	4.200941 × 10−30	4.200941 × 10−31	4.200941 × 10−32	4.200941 × 10−33
6	75%	2.25 × 108	4.501008 × 10−30	4.501008 × 10−31	4.501008 × 10−32	4.501008 × 10−33
7	80%	2.40 × 108	4.801075 × 10−30	4.801075 × 10−31	4.801075 × 10−32	4.801075 × 10−33
8	85%	2.55 × 108	5.101142 × 10−30	5.101142 × 10−31	5.101142 × 10−32	5.101142 × 10−33
9	90%	2.70 × 108	5.401209 × 10−30	5.401209 × 10−31	5.401209 × 10−32	5.401209 × 10−33
10	95%	2.85 × 108	5.701277 × 10−30	5.701277 × 10−31	5.701277 × 10−32	5.701277 × 10−33
11	99%	2.97 × 108	5.941330 × 10−30	5.941330 × 10−31	5.941330 × 10−32	5.941330 × 10−33

The analysis of the data unveiled a significant correlation between the spinning velocity of black holes and their temperature variation. It was observed that as the spinning

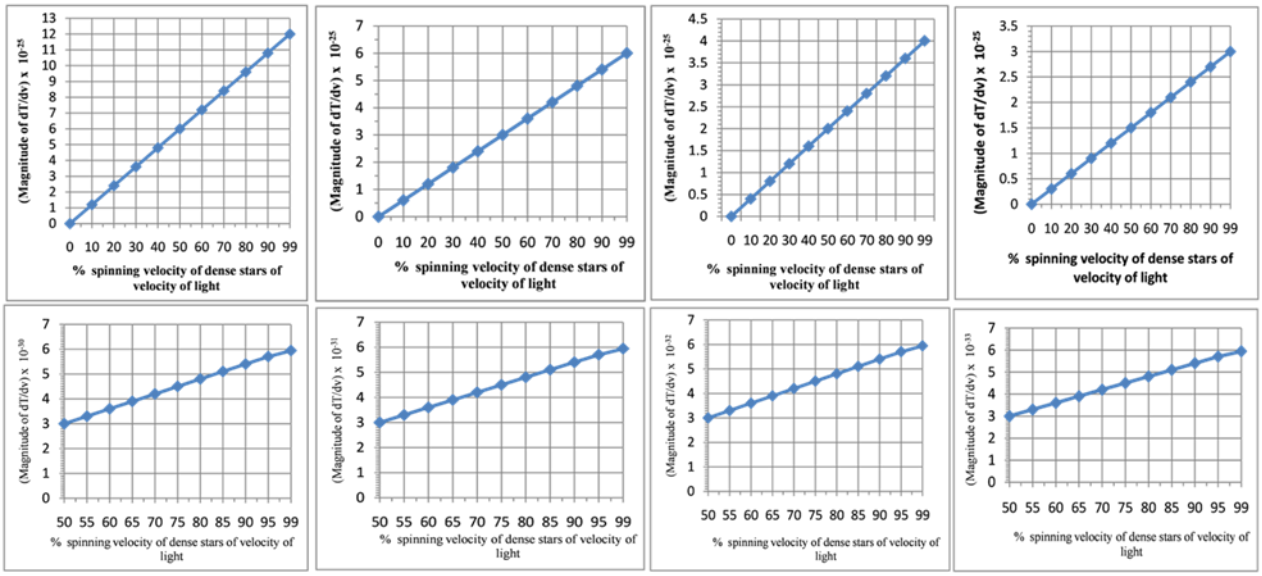

Figure 19 *The graph plotted between % spinning velocity of black holes of velocity of light and the rate of change of temperature of black holes w.r.t. spinning velocity for masses from* M=$5M_0$ *to* $M = 10^9 M_0$ *[20].*

velocity of black holes increases, the rate of change in temperature with respect to velocity also escalates. This finding shed light on the intricate relationship between the rotational properties of black holes and their thermal behavior, providing valuable insights into the underlying mechanisms governing these celestial phenomena [13], [20].

2.3 Singularity and gravitational wave

Massive stars undergo gravitational collapse when their nuclear fuel is depleted and cannot support their own weight against gravitational forces. As the core contracts under its own gravity, it reaches extreme densities and temperatures, leading to the formation of a dense core. The collapse continues until the core reaches a critical point where gravitational forces become infinitely strong and spacetime curvature becomes infinite. This point of infinite density and curvature is known as a singularity, which lies at the center of a black hole [5], [17].

In the context of General Relativity and black hole physics, the equation that describes a singularity at the center of a black hole is related to the spacetime metric and the curvature of spacetime. The singularity is typically characterized by the divergence of certain physical quantities, such as the density and curvature, to infinity. One of the key equations in General Relativity that describes the curvature of spacetime is the Einstein field equations, which can be written as:

$$G_\mu = 8\pi T_{\mu\nu}$$

where Gμν represents the Einstein tensor, which encodes the curvature of spacetime, and Tμν is the stress-energy tensor, which describes the distribution of matter and energy in spacetime [11].

Additionally, there are two gentler singularities: one falling inward from future infalling matter and the other flying upward from past scattered matter. Physicists aim to understand these singularities as they are governed by the laws of quantum gravity, which synthesize general relativity and quantum theory [15].

General relativity predicts that the dynamics near a singularity, especially during events like black hole mergers, can produce unique gravitational wave signatures that carry information about the nature of spacetime in extreme gravitational environments. By detecting and analyzing gravitational waves from such events, scientists can test the predictions of general relativity and explore the behavior of matter and energy near singularities. according to general relativity, singularities represent regions of spacetime where the curvature is infinitely strong, gravitational waves are disturbances in this curved spacetime, and the study of gravitational waves from extreme astrophysical events provides insights into the nature of singularities and the fundamental properties of gravity [15].

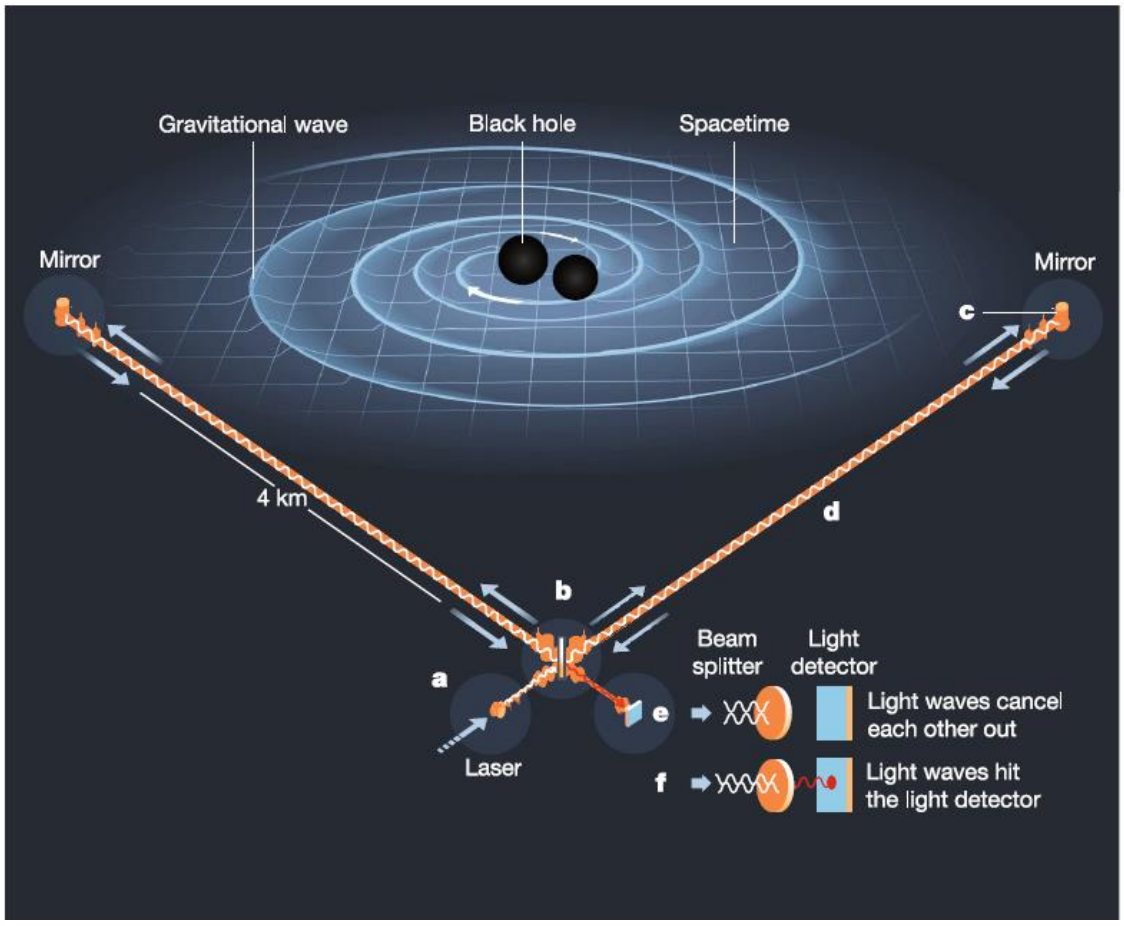

Figure 20 *Laser interferometers like LIGO and Virgo operate by splitting a laser beam into two perpendicular paths and then recombining them to detect tiny changes in the length of these paths caused by gravitational waves [17].*

Gravitational waves, originating from cataclysmic celestial events like the merger of black holes and neutron stars, are detectable phenomena observed by advanced gravitational-wave detectors such as LIGO. In September 2015, the twin Laser Interferometer Gravitational-wave Observatory (LIGO) detectors, managed by Caltech and MIT, achieved the groundbreaking feat of directly detecting gravitational waves for the first time. These waves were emitted during the collision of two black holes, affirming a prediction of Albert Einstein's general theory of relativity made a century earlier. Distinctive characteristics differentiate gravitational waves generated by black hole mergers and those produced by neutron star mergers, including the masses of the involved objects. Black hole mergers, occurring within the mass range of approximately 10^4M⊙-10^7M⊙ at galactic centers, are expected to produce gravitational waves in the millihertz band, potentially observable as bursts with lasting memory effects in pulsar timing data. In contrast, neutron star mergers involve objects of lower masses compared to black holes, resulting in discernibly different gravitational wave signatures [14], [15], [17].

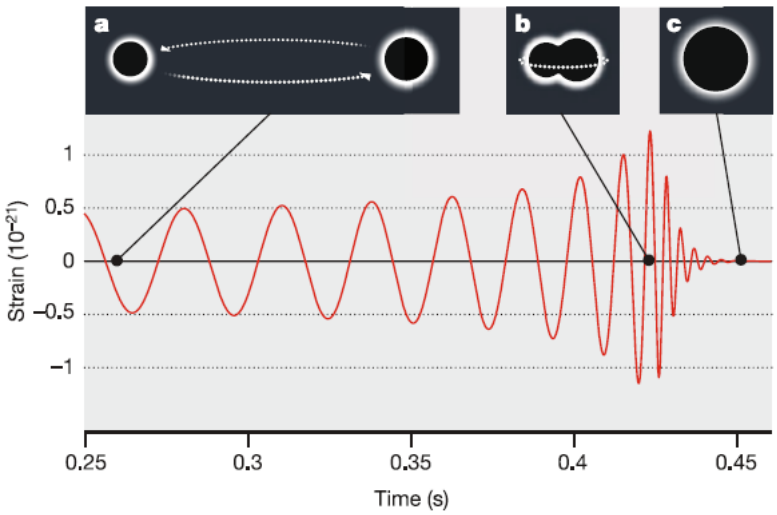

Figure 21 *Depiction of gravitational waves emanating from the merger of a binary black hole system.*

The diagram of figure above portrays the progression of gravitational waves originating from the merging of a binary black hole system. Initially, it shows two black holes in several orbits before their eventual fusion (a), followed by their merger at the critical moment (b). Afterward, the aftermath of the merger is depicted (c), indicating the remnant settling into its ultimate state as a solitary black hole. The vertical axis represents strain, which signifies the fractional alteration in the arm lengths of the LIGO detectors [15].

Valuable insights into the masses of black holes and neutron stars are provided by experimental observations. Direct measurements of these masses are obtained through gravitational-wave detections, facilitated by instruments like LIGO and Virgo, which detect gravitational waves emitted during cataclysmic events such as black hole

mergers and neutron star collisions. Additionally, electromagnetic observations across various wavelengths contribute to our understanding of these objects' masses. By studying the electromagnetic radiation emitted by black holes and neutron stars, astronomers can indirectly infer their masses. This approach complements the direct measurements obtained from gravitational-wave observations [14],[17].

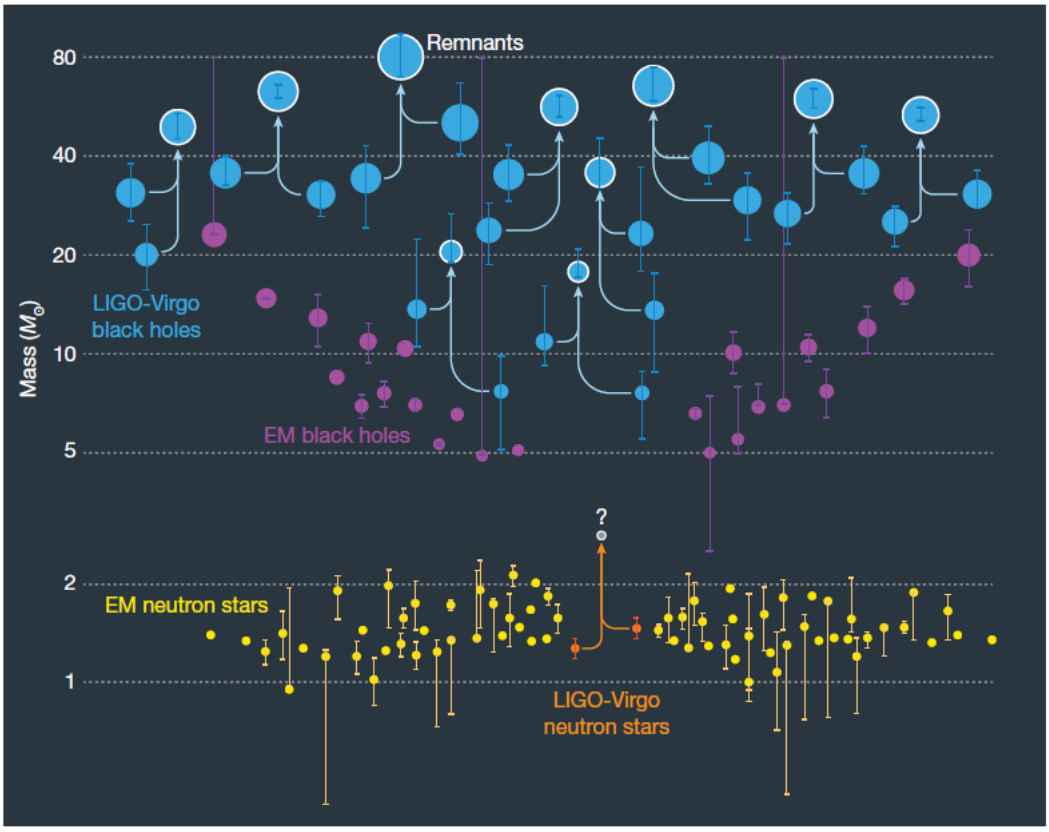

Figure 22 *Masses of black holes and neutron stars are determined through gravitational-wave detections and electromagnetic observations [17].*

The initial detection of the gravitational-wave signal GW150914 was achieved through low-latency searches for generic gravitational-wave transients. This means that the LIGO detectors were actively scanning the data in real-time to identify any potential gravitational-wave signals. The detection was reported within three minutes of data acquisition, highlighting the rapid response and analysis capabilities of the LIGO observatories. The initial detection of the gravitational-wave signal GW150914 was achieved through low-latency searches for generic gravitational-wave transients. This means that the LIGO detectors were actively scanning the data in real-time to identify any potential gravitational-wave signals. The detection was reported within three minutes of data acquisition, highlighting the rapid response and analysis capabilities of the LIGO observatories. This observation was made by the LIGO (Laser Interferometer Gravitational-Wave Observatory) Hanford, WA, and Livingston, LA, observatories simultaneously [15], [21].

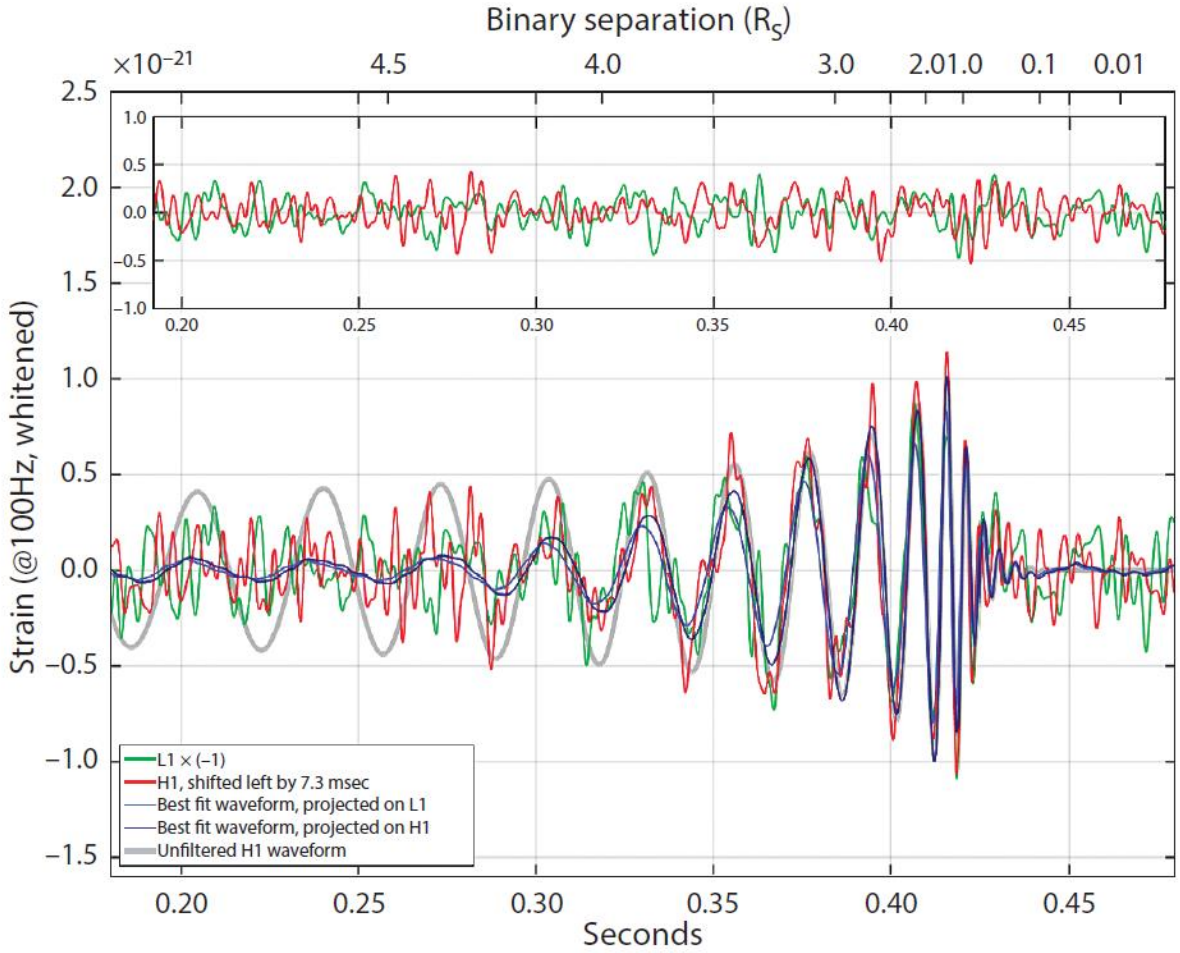

Figure 23 *The gravitational-wave event GW150914 observed by Advanced LIGO's Livingston, L1 (green) and Hanford, H1 (red) detectors, also showing best-fit templates computed by combining analytical and numerical activity [15].*

In gravitational-wave astronomy, strain refers to the fractional change in length experienced by an object when a gravitational wave passes through space. These waves cause a stretching and squeezing effect on objects, distorting the fabric of spacetime itself. Interferometric detectors like LIGO measure strain as the relative change in length of their arms induced by gravitational waves. As the waves pass through, they cause tiny oscillations in spacetime, leading to minuscule stretching and compression of the detector arms. Strain is dimensionless, representing a ratio of the change in length to the original length, and serves to quantify the amplitude of the gravitational wave's effect on the interferometer arms [21].

the detection of gravitational waves from the GW150914 event not only confirms the existence of these elusive phenomena but also provides a remarkable validation of the predictions of general relativity in describing the behavior of gravity and spacetime in the most extreme cosmic environments. The event stands as a testament to the enduring relevance and predictive power of Einstein's revolutionary theory of gravity [15], [21].

3. Discussion

The life cycle of stars culminates in the formation of black holes, which occurs when massive stellar cores collapse under their own gravity after exhausting their nuclear fuel. This process is governed by the principles of general relativity, which elucidate how massive objects distort the fabric of space-time. The resulting black holes possess such immense gravitational pull that not even light can escape, a phenomenon that confirms the predictions of general relativity. By studying black holes, scientists can push the boundaries of our understanding of gravity and gain deeper insights into the fundamental nature of the cosmos.

In this study, various techniques and models have been explored to analyze observational data related to black holes. Methods such as EHT-Imaging, Snapshot-Ring, DoG-HiT, and THEMIS Models contribute to capturing images, analyzing emission rings, enhancing features, and interpreting magnetospheric dynamics, allowing for the determination of linear and circular polarimetric images of synthetic models. Theoretical models, such as the Magnetically Arrested Disk (MAD) and Standard and Normal Evolution (SANE) models based on general relativity, guide the interpretation of observational data and offer predictions about the appearance of black hole event horizons and surrounding emissions.

Furthermore, this study sheds light on recent findings concerning the polarization of the emission ring around Sgr A*, providing valuable insights into the magnetic field geometry near the event horizon of the supermassive black hole. Additionally, the concept of Hawking radiation and its associated theoretical temperature, known as the Hawking temperature, are discussed, highlighting the relevance of gravitational-wave astronomy. The detection of gravitational waves from black hole mergers and the confirmation of binary black hole systems through observations made by instruments like LIGO and Virgo underscore the significance of ongoing efforts to explore and understand these enigmatic cosmic phenomena.

4. Conclusion

The life cycle of stars culminates in the formation of black holes, governed by general relativity, where massive cores collapse under gravity. These black holes possess immense gravitational pull, confirming general relativity's predictions. Various techniques and models, including EHT-Imaging and theoretical models like MAD, aid in analyzing observational data. Recent findings on polarization around Sgr A* offer insights into black hole magnetospheric dynamics. While Hawking radiation and its associated Hawking temperature remain pivotal in understanding black hole physics. The detection of gravitational waves from black hole mergers underscores ongoing efforts in understanding these phenomena.

Reference

[1] Ward-Thompson, D. and Whitworth, A.P. (2015). *An introduction to star formation*. Cambridge: University Press.

[2] Stahler, S.W. and Palla, F. (2008). *The Formation of Stars*. John Wiley & Sons.

[3] J. Stayner, "large.stanford.edu," 25 5 2017. [Online]. Available: http://large.stanford.edu/courses/2017/ph241/stayner2/ . [Accessed 19 1 2024].

[4] Schulz, N.S. (2007). From Dust To Stars. Springer Science & Business Media.

[5] K. R. Lang, the life and death of stars, New York: Cambridge university, 2013.

[6] NASA (2014). Stars - Introduction. [online] Nasa.gov. Available at: https://imagine.gsfc.nasa.gov/science/objects/stars1.html. [Accessed 1 1 2024].

[7] D. Moiraf, "The use of Plasma Mirror for Relativistic Electron Generation Relevant to Fast Ignition in Inertial Confinement Fusion," Research Gate, Toulouse, 2020.

[8] Natario, J. (2011). *General Relativity Without Calculus*. Springer Science & Business Media.

[9] Dreyer, O., Kelly, B.J., Krishnan, B., Lee Samuel Finn, Garrison, D.L. and Lopez-Aleman, R. (2004). Black-hole spectroscopy: testing general relativity through gravitational-wave observations. *Classical and Quantum Gravity*, 21(4), pp.787–803. doi: https://doi.org/10.1088/0264-9381/21/4/003.

[10] sci.esa.int. (2015). *ESA Science & Technology - Spacetime curvature*. [online] Available at: https://sci.esa.int/web/lisa-pathfinder/-/56434-spacetime-curvature. [accessed Mar. 14, 2024].

[11] Psaltis, D. (2019). Testing general relativity with the Event Horizon Telescope. *General Relativity and Gravitation*, 51(10). doi: https://doi.org/10.1007/s10714-019-2611-5.

[12] Akiyama, K., Alberdi, A., Alef, W., Asada, K., Azulay, R., Baczko, A.-K., Ball, D., Baloković, M., Barrett, J., Bintley, D., Blackburn, L., Boland, W., Bouman, K.L., Bower, G.C., Bremer, M., Brinkerink, C.D., Brissenden, R., Britzen, S., Broderick, A.E. and Broguiere, D. (2019). First M87 Event Horizon Telescope Results. V. Physical Origin of the Asymmetric Ring. *The Astrophysical Journal*, [online] 875(1), p.L5. doi: https://doi.org/10.3847/2041-8213/ab0f43.

[13] Hawking, S.W. (1972). Black holes in general relativity. *Communications in Mathematical Physics*, 25(2), pp.152–166. doi: https://doi.org/10.1007/bf01877517.

[14] Narlikar, J.V. (2010). *An Introduction to Relativity*. Cambridge University Press.

[15] Buchwald, J.Z. (2020). *Einstein was right : the science and history of gravitational waves*. Princeton, New Jersey: Princeton University Press.

[16] Fine Art America. (2023). *Black Hole #10 by Mark Garlick/science Photo Library*. [online] Available at: https://fineartamerica.com/featured/10-black-hole-mark-garlickscience-photo-library.html. (accessed Mar. 16, 2024).

[17] Miller, M.C. and Yunes, N. (2019). The new frontier of gravitational waves. *Nature*, 568(7753), pp.469–476. doi: https://doi.org/10.1038/s41586-019-1129-z.

[18] M. CARLISLE , C. (2019). *Scientists Unveil First Black Hole Image*. [online] Sky & Telescope. Available at: https://skyandtelescope.org/astronomy-news/black-holes/scientists-unveil-first-black-hole-image/. (accessed Mar. 16, 2024)

[19] Temming, M. (2020). *EHT data show turbulence makes the glowing ring around M87's black hole wobble*. [online] Science News. Available at: https://www.sciencenews.org/article/event-horizon-eht-data-m87-black-hole-turbulence-wobble. (Accessed: 05 April 2024).

[20] Dipo Mahto, Ranjan, A. and Krishna Murari Singh (2017). Relativistic Variation of Black Hole Temperature with Respect to Velocity in XRBs and AGN. International Journal of Astronomy and Astrophysics, 07(01), pp.1–10. Doi: https://doi.org/10.4236/ijaa.2017.71001.

[21] Abbott, B. P., Abbott, R., Abbott, T. D., Abernathy, M. R., Acernese, F., Ackley, K., Adams, C., Adams, T., Addesso, P., Adhikari, R. X., Adya, V. B., Affeldt, C., Agathos, M., Agatsuma, K., Aggarwal, N., Aguiar, O. D., Aiello, L., Ain, A., Ajith, P. and Allen, B. (2016). Observation of Gravitational Waves from a Binary Black Hole Merger. Physical Review Letters, 116(6). Doi: https://doi.org/10.1103/physrevlett.116.061102.